Impact of Band Non-parabolicity on the Onset Voltage in a Nanowire Tunnel Field-effect Transistor

H. Carrillo-Nuñez[1], W. Magnus[2,3], William G. Vandenberghe[4], Bart Sorée[2,3] and F. M. Peeters[2]
[1]IM2NP, UMR CNRS 7334, Bat. IRPHE, Technopôle de Château-Gombert, 13384 Marseille, France
[2]Departement Fysica, Universiteit Antwerpen, Groenenborgerlaan 171, B-2020 Antwerpen, Belgium
[3]imec, Kapeldreef 75, B-3001, Leuven, Belgium
[4]University of Texas at Dallas, Department of Materials Science and Engineering, Richardson, Texas 75080, USA
email: hamilton.carrillo@im2np.fr

***Abstract*—The phonon-assisted band-to-band tunneling (BTBT) current has been computed for a cylindrical nanowire tunneling field-effect transistor (TFET) with an all-round gate covering the source region. Although we have considered relatively thick wires, i.e. diameters ranging between 5 and 8 nm, we found that BTBT is considerably affected by the carrier confinement in the radial direction. Therefore, a self-consistent solution of the Schrödinger and Poisson equations must be carried out. For the latter, we have implemented a non-linear variational principle based on the modified local density approximation taking into account non-parabolic corrections for both conduction and valence bands. Our findings show not only that the confinement effects in nanowire TFETs have a stronger impact on the onset voltage of the tunneling current in comparison with their planar counterparts but also that the value of the onset voltage is overestimated when the valence band nonparabolicity is ignored.**

I. Introduction

Over the last decades, the tunneling field-effect transistor (TFET), based on band-to-band tunneling (BTBT), has become a potential candidate to outperform a conventional metal-oxide-semiconductor field-effect transistor (MOSFET) as it is expected to improve on the 60 mV/dec sub-threshold slope of nanometer-sized MOSFETs. Therefore, in the recent past, the optimization of the TFETs working principle has been the aim of numerous studies, and various configurations, such as the reverse-bias $p-i-n$ diode with a gate surrounding the intrinsic region, [1], [2] have been proposed. Ref. [2] investigates BTBT occurring in the longitudinal direction, near the $p-i$ junction where the conduction band (CB) and valence band (VB) start to overlap.

In this work, however, we have considered relatively thick Si cylindrical nanowire TFETs having diameters between 5 and 8 nm and an all-round gate covering the $p^{++}-$doped source region (see Fig. 1), in analogy with their planar counterparts [3]. For the latter it was found that, under high gate bias, a tunnel current emerges due to radial confinement, being proportional to the gate length and referred to as line tunneling current. In Ref. [3], carrier confinement was observed to have a strong impact on the onset voltage of a planar device but, although confinement is expected to be even more pronounced in a nanowire, there have been no systematic studies of the confinement related onset shift in nanowire TFETs. In this light, we have thoroughly investigated the effect of confinement in a $p-i-n$ Si nanowire TFET, first within the effective mass approximation and afterwards with inclusion of non-parabolic corrections for the CB [4] and VB [5].

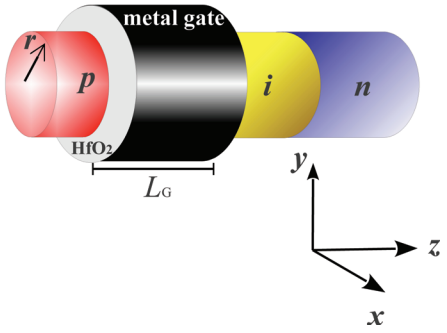

Fig. 1. Cylindrical nanowire TFET with an all-around gate on top of the source.

In addition, BTBT, mediated by the electron-phonon interaction in indirect semiconductors, has been treated according to the perturbative approach introduced in Ref. [6], which we have extended to the case of nanowire TFETs. The corresponding transport formalism enabling us to deal with high electric fields that appear in the one-electron Schrödinger equation for both the VB and CB, was successfully combined with the implementation of a non-linear variational principle based on the modified local density approximation (MLDA) [7], [8]. Applied originally to conventional nanowire MOSFETs [8], the MLDA has substantially reduced the computational complexity of the Poisson-Schrödinger solver treating radial confinement.

In section II we summarize the procedure to compute the carrier concentrations including the non-parabolic corrections for the CB and VB, within the MLDA-based variational approach, whereas section III provides the expressions for the tunneling current and the MLDA-based tunneling probability. In section IV, we briefly discuss our main results while the conclusions of this paper are presented in section V.

II. Band nonparabolicity within the framework of the MLDA

For the nanowire TFET shown in Fig. 1, we have assumed a [100]-oriented perfect cylindrical wire. Adopting the effective mass approximation, the kinetic energy operator for the electrons in the VB (CB) can be written in cylindrical coordinates (r,ϕ,θ) as

$$\hat{T}_{\mathrm{v(c)}\alpha} = \pm\frac{\hbar^2}{2m_{\mathrm{v(c)}\alpha z}}\frac{\partial^2}{\partial z^2} \pm \frac{\hbar^2}{2m_{\mathrm{v(c)}\alpha\perp}}\left(\frac{\partial^2}{\partial r^2}+\frac{1}{r}\frac{\partial}{\partial r}+\frac{1}{r^2}\frac{\partial^2}{\partial\phi^2}\right). \quad (1)$$

978-1-4673-5736-4/13/$31.00 ©2013 IEEE

α is a valley index labeling the six conduction band valleys as well as the light and heavy hole valleys of the VB whereas $m_{\mathrm{v(c)}\alpha\perp} = 2m_{\mathrm{v(c)}\alpha x}m_{\mathrm{v(c)}\alpha y}\,/(m_{\mathrm{v(c)}\alpha x} + m_{\mathrm{v(c)}\alpha y})$ and $m_{\mathrm{v(c)}\alpha z}$ respectively denote the effective masses in the planar cross-section of the wire and the longitudinal mass the in z-direction. Accordingly, the one-electron Hamiltonian for the α-th VB can be expressed as [5]

$$H_{\mathrm{v}\alpha} = \hat{T}_{\mathrm{v}\alpha}\,\chi_{\alpha}\big(-E - eV(r,z) - E_{\mathrm{g}}\big) - eV(r,z) \qquad (2)$$

where the function $\chi_{\mathrm{L(H)}}(E)$ models the light (heavy) hole VB nonparabolicity [5]. On the other hand, we use Kane's model in order to incorporate nonparabolicity [4] in the α-th CB,

$$H_{\mathrm{c}\alpha}\Psi_{\mathrm{c}\alpha}(\mathbf{r}) = \Big[E + \gamma\big(E + eV(r,z)\big)^2\Big]\,\Psi_{\mathrm{c}\alpha}(\mathbf{r}), \qquad (3)$$

taking the nonparabolicity coefficient γ to be 0.5 eV^{-1}. The electrostatic potential $V(r,z)$ obeys Poisson equation,

$$\nabla^2 V(r,z) = -\frac{1}{\epsilon}\,\rho(r,z), \qquad (4)$$

under the assumption that all carriers are confined to interior of the wire, i.e. the barrier potential energy at the semiconductor/oxide interface ($r = R$) is taken to be infinitely high.

The calculation of the carrier concentration in both the CB and VB involves the self-consistent solution of the 3D Schrödinger and Poisson equations which, in principle, can be obtained by carrying out consecutive iterations of (2)-(4) until convergence is reached. However, in this work, we have adopted the MLDA-based variational approach [8] to establish the charge and potential profiles inside the nanowire TFET. In particular, we have extended the MLDA-based approach to properly incorporate the radial confinement that underlies the line tunneling current. This is accomplished by considering, as a first step, a potential $V_1(r)$ corresponding to an all-round biased gate which is long enough to neglect the z-dependence of $V(r,z)$ while the wave functions $R_{\nu\mathrm{v(c)}}(r)\mathrm{e}^{\mathrm{i}m\phi}$ and the corresponding subband energies $W_{\nu\mathrm{v(c)}}$ are computed within the effective mass approximation. Next, implementing the strategy adopted by Jin *et-al* in Ref. [4], we use first-order perturbation theory to calculate an explicit expression for the non-parabolic dispersion relations by inserting the diagonal matrix elements $V_{1,\nu\mathrm{v(c)}} = \int_0^R \mathrm{d}r\, r|R_{\nu\mathrm{v(c)}}(r)|^2\, V_1(r)$ into the non-parabolic Schrödinger equations, thereby obtaining,

$$E^{\mathrm{NP}}_{\nu\mathrm{c}}(k) \approx E_{\mathrm{g}} - eV_{1,\nu\mathrm{c}} + \frac{1}{2\gamma}\left[\sqrt{1 + 4\gamma\left(\frac{\hbar^2k^2}{2m_{\mathrm{c}\alpha z}} + W_{\nu\mathrm{c}} + eV_{1,\nu\mathrm{c}}\right)} - 1\right], \qquad (5)$$

$$E^{\mathrm{NP}}_{\nu\mathrm{v}}(k) \approx -\left(\frac{\hbar^2k^2}{2m_{\mathrm{v}\alpha z}} + W_{\nu\mathrm{v}} - eV_{1,\nu\mathrm{v}}\right) \times \chi_{\mathrm{v}\alpha}\big(-E^{\mathrm{NP}}_{\nu\mathrm{v}}(k) - eV_{1,\nu\mathrm{v}}\big) - eV_{1,\nu\mathrm{v}} \qquad (6)$$

for the CB and VB, respectively. Now, we invoke the MLDA by adding the correction potential $V_2(r,z) = V(r,z) - V_1(r)$ to the energy arguments of the non-parabolic local density of states, $A_{\mathrm{v(c)}}(\mathbf{r},\mathbf{r};E) = \sum_\nu A^{\mathrm{NP}}_{\nu\mathrm{v(c)}}(r,z;E + eV_2(r,z))$, the z-dependence of which reflects the finite gate length. As an immediate consequence of the MLDA, the total charge density containing the contributions of electrons in the conduction and valence bands, emerges as a local functional of $V_2(r,z)$, i.e.,

$$\rho[r,V_2(r,z)] = e\Big(n_{\mathrm{v}}[r,V_2(r,z)] - n_{\mathrm{c}}[r,V_2(r,z)] - N_{\mathrm{A}}\Big), \qquad (7)$$

N_{A} being the acceptor concentration, whereas the concentration of electrons $n_{\mathrm{c(v)}}$, occupying the conduction (valence) subbands inside the nanowire TFET, is expressed within the MLDA as

$$n_{\mathrm{c(v)}}(r,z) = \frac{1}{\pi}\sum_\nu \big|R_{\nu\mathrm{c(v)}}(r)\big|^2 \int \mathrm{d}k\, \mathcal{F}_{\mathrm{c(v)}}\big(E^{\mathrm{NP}}_{\nu\mathrm{c(v)}}(k) - eV_2(r,z)\big), \qquad (8)$$

with $\mathcal{F}_{\mathrm{c}}(E) = f_{\mathrm{c}}(E)$ and $\mathcal{F}_{\mathrm{v}}(E) = 1 - f_{\mathrm{v}}(E)$. $f_{\mathrm{c}}(E)$ and $f_{\mathrm{v}}(E)$ respectively denote the Fermi-Dirac distribution functions for the CB and VB incorporating the effect of the applied source/drain voltage. As explained in detail in in Ref. [8], the formal structure of both concentrations appearing in (7) and (8) as local functionals of $V_2(r,z)$, is the key ingredient to construct a non-linear action functional for the electrostatic potential, the numerical minimization of which yields a simultaneous solution of the Poisson and Schrödinger equations, within the restrictions of the MLDA.

III. Phonon assisted BTBT current within the MLDA

Once the self-consistent solution to the Schrödinger and Poisson equations is obtained, the resulting electrostatic potential profile $V(r,z)$ enables the application of the MLDA to calculate the probabilities for BTBT mediated by the absorption or emission of phonons [3]. Indeed, since also the spectral functions for both bands appear to be local functionals w.r.t. their dependence on the correcting potential $V_2(r,z)$, we may write the BTBT transmission probabilities as

$$\begin{aligned} T^{\mathrm{abs,em}}_{\mathrm{v}}(E) &= \Omega\,|M'_{\mathbf{k}_0}|^2 \sum_{\nu,\nu'}\int_0^R \mathrm{d}r\, r R^2_{\nu\mathrm{c}}(r) R^2_{\nu'\mathrm{v}}(r) \\ &\quad\times \int_0^{L_{\mathrm{G}}} \mathrm{d}z\, A^{\mathrm{NP}}_{\nu'\mathrm{v}}\left(z,z;E + eV_2(r,z)\right) \\ &\quad\times A^{\mathrm{NP}}_{\nu\mathrm{c}}\left(z,z;E + eV_2(r,z) \pm \hbar\omega_{\mathbf{k}_0}\right) \\ &\equiv \sum_{\nu,\nu'}\int_0^R \mathrm{d}r\, r R^2_{\nu\mathrm{c}}(r) R^2_{\nu'\mathrm{v}}(r)\, T^{\mathrm{abs,em}}_{\nu\nu'\mathrm{v}}(r;E), \end{aligned} \qquad (9)$$

where $\Omega|M'_{\mathbf{k}_0}|^2$ is the electron-phonon strength for a phonon with energy $\hbar\omega_{\mathbf{k}_0}$ that bridges the electron transition between the highest valence subbands and the lowest conduction subbands. Then, the phonon-assisted line current density can be

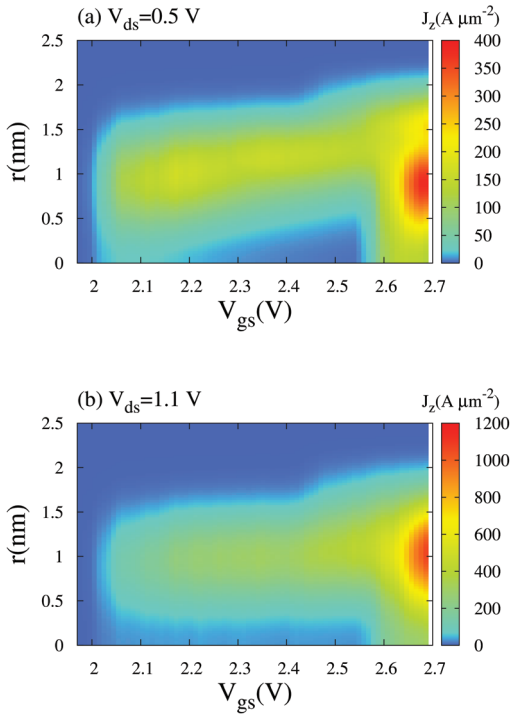

Fig. 2. Contour plot of the current densities as function of $V_{\rm gs}$ and r inside the nanowire TFET of radius $R = 2.5$ nm. The applied drain voltages are (a) $V_{\rm ds} = 0.5$ V, (b) $V_{\rm ds} = 1.1$ V.

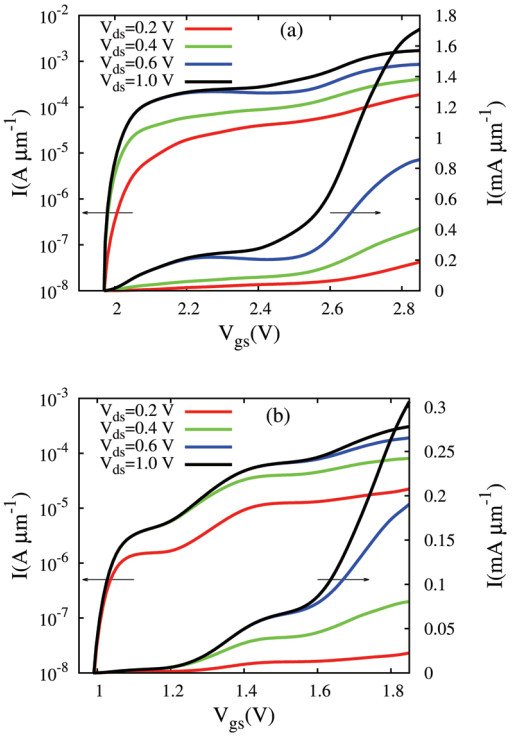

Fig. 3. Line tunneling current as function of the gate voltage for different $V_{\rm ds}$ in case of a nanowire TFET of radius (a) $R = 2.5$ nm and (b) $R = 4$ nm. The vertical axis represents the tunneling current per unit gate length.

computed from [3], [6]

$$J_z(r) = -\frac{2e}{\hbar}\sum_{\nu,\nu'} R^2_{\nu{\rm c}}(r)R^2_{\nu'{\rm v}}(r)\int\frac{{\rm d}E}{2\pi}$$
$$\times\Big[\Big(f_{\rm v}(E)(1-f_{\rm c}(E-\hbar\omega_{\mathbf{k}_0}))(\nu(\hbar\omega_{\mathbf{k}_0})+1)$$
$$-f_{\rm c}(E-\hbar\omega_{\mathbf{k}_0})(1-f_{\rm v}(E))\nu(\hbar\omega_{\mathbf{k}_0})\Big)T^{\rm em}_{\nu\nu'{\rm v}}(r;E)$$
$$+\Big(f_{\rm v}(E)(1-f_{\rm c}(E+\hbar\omega_{\mathbf{k}_0}))\nu(\hbar\omega_{\mathbf{k}_0})$$
$$-f_{\rm c}(E+\hbar\omega_{\mathbf{k}_0})(1-f_{\rm v}(E))(\nu(\hbar\omega_{\mathbf{k}_0})+1)\Big)T^{\rm abs}_{\nu\nu'{\rm v}}(r;E)\Big]. \quad (10)$$

In the latter, $\nu(E) = (\exp(\beta E)-1)^{-1}$ is the Bose-Einstein distribution function and $\beta = 1/k_{\rm B}T$. Note that $J_z(r)$ depends only on r, thus complying with the requirement that a stationary current be solenoidal. Finally, the line tunneling current is obtained by integrating over the cross section of the nanowire, i.e. $I = 2\pi\int_0^R {\rm d}r\, r J_z(r)$.

IV. Results and Discussion

For the simulations, we have considered Si nanowires with diameters ranging between 5 nm and 8 nm. The six [100] oriented conduction band valleys are characterized by their longitudinal mass $m_l = 0.916\, m_0$ and transverse mass $m_t = 0.19\, m_0$, whereas the heavy and light hole masses of the valence band are respectively taken to be $m_{hh} = 0.49\, m_0$ and $m_{lh} = 016\, m_0$. In all cases the gate length equals $L_{\rm G} = 20$ nm, while room temperature conditions are assumed. The following material parameters have been used for the results presented below: $E_{\rm g} = 1.12$ eV, $\epsilon_{\rm s} = 11.5\epsilon_0$, $\epsilon_{\rm ox} = 15\epsilon_0$, $t_{\rm ox} = 1$ nm. The acceptor doping concentration and the phonon energy are respectively chosen to be $N_{\rm A} = 10^{20}$ cm^{-3} and $\hbar\omega_{\mathbf{k}_0} = 18.4$ meV. Accordingly, the electron-phonon strength is given by $\Omega|M'_{\mathbf{k}_0}|^2 = 4.86\times10^{-25}$eV^{2}cm^3. When a positive gate voltage is applied, i.e. $V_{\rm gs} > 0$, the mobile holes are repelled towards the center of the nanowire while the electrons are piling up near the semiconductor/oxide interface, thereby forming a $n-$channel. Although the electron concentration was found to be much higher than the hole concentration, there is a substantial spatial overlap of both profiles which is reflected in the increased BTBT probability. The latter is confirmed by the contour plot of the phonon-assisted BTBT current density shown in Fig. 2 as a function of $V_{\rm gs}$ and r for two different values of the source/drain voltage $V_{\rm ds}$, revealing that the current density is mainly concentrated in the overlap region $r \leqslant 2$nm. Furthermore, in Fig. 2 we observe that the onset voltage for BTBT, and hence for its corresponding line tunneling current, reaches the rather high value of $V_{\rm gs} = 1.97$ V which is a consequence of strong carrier confinement which is expected to lift up the subband energies in the CB while pulling down the VB subband energies. Therefore, in order to access to the first few electron and hole subbands, a higher onset voltage needs be applied in comparison to the case of the planar line tunneling current structures [3].

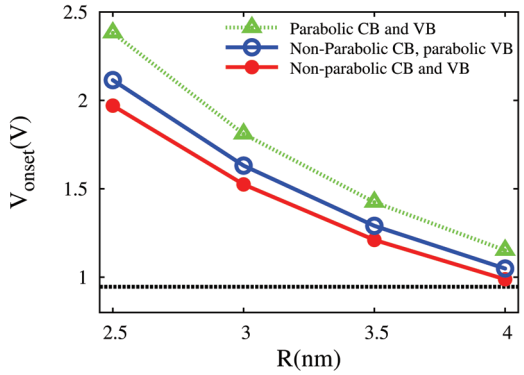

(a)

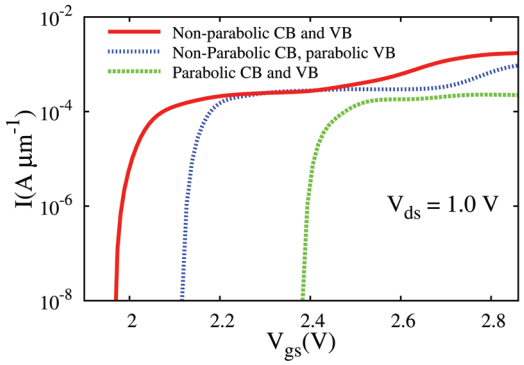

(b)

Fig. 4. (a) Onset voltage as a function of the nanowire radius. The horizontal black line represents the onset voltage of the planar TFET discussed in Ref. [3]. Different cases are considered: 1) parabolic CB and VB, 2) only a non-parabolic CB and 3) nonparabolic CB and VB. (b) Comparison of the parabolic and nonparabolic line tunneling current for $R = 2.5$ nm. In all cases $V_{\rm ds} = 1$ V.

In Figs. 3(a) and 3(b), the line tunneling current is plotted as a function of $V_{\rm gs}$ for two nanowire TFETs with radii $R = 2.5$ nm and $R = 4$ nm, respectively. As a first observation, the onset voltage of the thinner nanowire is found to be approximately 1.97 V, whereas it is reduced to 1 V for the thicker nanowire, thereby approaching the onset voltage of the planar TFET found in Ref. [3]. The latter is expected since the confinement effect is less pronounced in the thicker wire, while its band structure is more bulk-like. Secondly, in both cases the current increases rapidly, while attaining different saturation levels for higher values of $V_{\rm gs}$. The saturation plateaus can be ascribed to transitions of electrons between higher conduction and lower valence subband levels, typically emerging with increasing gate voltage. On the other hand, from Fig. 3, we may infer the dependence of the onset voltage on the nanowire radius which is confirmed by Fig. 4(a), explicitly depicting the effect of the confinement on the onset voltage in nanowire TFETs. Clearly, in order to line up the lowest conduction subband and the highest valence subband, a larger gate voltage is needed, as observed in Fig. 4(a) The latter also illustrates how the inclusion of non-parabolicity corrections may degrade the onset voltage, thereby mitigating the effect of confinement. In particular, it turns out that a full parabolic and a full non-parabolic treatment of both the CB and VB give rise to an onset voltage difference of approximately 0.4 V for the thinnest nanowire TFET. Moreover, neglect of the valence band nonparabolicity leads to an overestimated onset voltage, even for the thickest wire considered in this work.

Finally, for sake of completeness, Fig. 4(b) shows the tunneling current for the following cases: parabolic CB and VB, only non-parabolic CB, and non-parabolic CB and VB, with $V_{\rm ds} = 1$ V in all three cases. Within the range shown here, the parabolic line tunneling not only has a higher onset voltage but its intensity is also found to be smaller than in the corresponding non-parabolic cases. Indeed, since the non-parabolic CB (VB) subband energies are lower (higher) than their parabolic counterparts, the effective bandgap is lowered, while more subbands are occupied, thus contributing to the current.

In summary, using the MLDA-based variational approach introduced earlier in Ref. [8], we have solved self-consistently the Schrödinger and Poisson equations to study the phonon-assisted BTBT in a nanowire TFET. Then, having expressed the BTBT probability and its corresponding current density within the MLDA, the line tunneling current has been computed for different nanowire radii, whereas non-parabolic corrections for both the CB and VB were included. We have found that carrier confinement in nanowire TFETs has a strong impact on the onset voltage in comparison with the case of planar TFET. Also, since a full parabolic treatment of the bands overestimates the onset voltage, the inclusion of non-parabolic corrections is crucial to predict the performance of Si-based nanowire TFETs, especially in the case of thin nanowires.

This work was supported by the Flemish Science Foundation (FWO-VI) and the Interuniversity Attraction Poles, Belgium State, Belgium Science Policy, and imec Leuven. H.C-N would like to thank the French funding agency CNRS for the financial support at the last stage of this work.

References

[1] S. K. Banerjee, W. Richardson, J. Coleman, and A. Chatterjee, "A new three-terminal tunnel device," *IEEE Elec. Dev. Lett.*, vol. 8, pp. 347–349, 1987.

[2] A. S. Verhulst, B. Sorée, D. Leonelli, W. G. Vandenberghe, and G. Groeseneken, "Modeling the single-gate, double-gate, and gate-all-around tunnel field-effect transistor," *J. App. Phys.*, vol. 107, pp. 024 518–024 526, 2010.

[3] W. G. Vandenberghe, B. Sorée, W. Magnus, G. Groeseneken, and M. V. Fischetti, "Impact of field-induced quantum confinement in tunneling field-effect devices," *App. Phys. Lett.*, vol. 98, p. 143503, 2011.

[4] S. Jin, M. V. Fischetti, and T.-W. Tang, "Modeling of electron mobility in gated silicon nanowires at room temperature: Surface roughness scattering, dielectric screening, and band nonparabolicity," *J. App. Phys.*, vol. 102, p. 083715, 2007.

[5] S. Rodríguez-Bolivar, F. M. Gómez-Campos, and J. E. Carceller, "Simple analytical valence band structure including warping and non-parabolicity to investigate hole transport in si and ge," *Semincond. Sci. Technol.*, vol. 20, pp. 16–22, Nov. 2005.

[6] W. G. Vandenberghe, B. Sorée, W. Magnus, and M. V. Fischetti, "Generalized phonon-assisted zener tunneling in indirect semiconductors with non-uniform electric fields: A rigorous approach," *J. App. Phys.*, vol. 109, p. 124503, 2011.

[7] G. Paasch and H. Übensee, "A modified local density approximation: Electron density in inversion layers," *Phys. Status Solidi B*, vol. 113, pp. 165–178, 1982.

[8] H. Carrillo-Nuñez, W. Magnus, and F. M. Peeters, "A simplified quantum mechanical model for nanowire transistors based on non-linear variational calculus," *J. App. Phys.*, vol. 108, p. 063708, 2010.